Spacecraft Attitude Control with Saturation and Attitude Forbidden Constraints via Second‐Order Cone Programming

CHEN Xi[1], *CAO Ruihao*[2], *HU Qinglei*[1,3*]

1. School of Automation Science and Electrical Engineering, Beihang University, Beijing 100191, P.R. China;

2. Xi'an Flight Automatic Control Research Institute, Aviation Industry Corporation of China, Xi'an 710076, P.R. China;

3. Beijing Advanced Innovation Center for Big-Data Based Precision Medicine, Beihang University, Beijing 100191, P.R. China

Abstract: This paper investigates the optimal control problem of spacecraft reorientation subject to attitude forbidden constraints, angular velocity saturation and actuator saturation simultaneously. A second-order cone programming (SOCP) technology is developed to solve the strong nonlinear and non-convex control problem in real time. Specifically, the nonlinear attitude kinematic and dynamic are transformed and relaxed to a standard affine system, and linearization and L1 penalty technique are adopted to convexify non-convex inequality constraints. With the proposed quadratic performance index of angular velocity, the optimal control solution is obtained with high accuracy using the successive SOCP algorithm. Finally, the effectiveness of the algorithm is validated by numerical simulation.

Key words: spacecraft reorientation; attitude forbidden constraints; actuator saturation; velocity saturation; second-order cone programming (SOCP)

0　Introduction

The constrained attitude reorientation of rigid spacecraft has gained immense popularity in recent years. Some light-sensitive payloads, such as infrared telescope and interferometers, should not be directly exposed to some bright objects, leading to attitude forbidden zones during the maneuvering. Due to the measurement range limit of the equipped sensors, the spacecraft can only maneuver in a lower angular velocity. Moreover, the actuators, such as flywheels and moment gyroscopes, cannot provide any requested control torques due to its physical limitations, which may lead to actuators' saturation. In a realistic scenario, all these issues may cause considerable difficulties in the design of attitude control algorithm for meeting high precision pointing requirement and desired control performance during the missions, especially when all these constraints are considered simultaneously.

Several nonlinear methods have been proposed to handle the spacecraft reorientation problem with attitude constraints, such as artificial potential function (APF)[1-4], path planning[5-7], and model predictive control (MPC) methods[8]. However, most of the above methods can only guarantee the feasibility rather than optimality, so the optimal control problem is supposed to be considered. As a class of convex optimization, second-order cone programming (SOCP) can avoid this defect effectively[9-10]. Kim et al.[11-12] aimed to settle the attitude constraints during the spacecraft maneuvering. Wherein, the Schur supplementary formula was applied to

solve the dynamic constraints. It should be noted that most practical problems do not naturally satisfy the requirements of the SOCP. Therefore, several relevant attempts have been proposed. In Refs.[13-14], the constraints in trajectory planning problems were disposed by lossless convexification to satisfy the requirements of standard SCOP framework, and a proper performance index was designed to keep the equivalence. In order to solve the optimal attitude control problem for spacecraft, a semidefinite relaxation method was introduced in Refs.[15-16], and the convergence of the problem was analyzed. The work in Ref.[17] proposed a SOCP method to solve a class of non-convex optimal problems, where the non-convexity was caused by concave state constraints and nonlinear equality constraints. Refs.[18-19] focused on the optimal problems with linear or quadratic state constraints and non-convex control constraints. The original problem was relaxed by slack variables, and the transformed problem could have the same solution with the original problem.

Other practical problems during the spacecraft reorientation maneuvering are angular velocity saturation and actuator saturation. The occurrence of these saturations can lead to substantial performance deterioration. As such, several control schemes have been proposed to deal with saturation constraints. Ref.[20] designed a control algorithm that considered both angular velocity and actuator saturation. The adaptive control algorithm in Ref.[21] also focused on the spacecraft control problem with actuator and velocity constraints. In Ref.[22], the angular velocity constraint was addressed by using the barrier Lyapunov function. The authors in Refs.[23-25] devoted to the nonlinear MPC method based on SO(3). The designed controllers could ensure that the angular velocity was limited within the set bound while completing the reorientation task.

Motivated by the above discussions, this paper intends to solve the optimal attitude control for spacecraft reorientation with attitude forbidden constraints and saturation constraints based on the SOCP algorithm. The contributions are highlighted as follows:

(1) The great challenge are the strongly nonlinear attitude dynamics and concave constraints. Thus, great efforts are devoted to transform the original into SOCP framework by relaxation and convexification. Specially, the nonlinear attitude dynamics are transformed and relaxed to a standard control affine system, and linearization and L1 penalty technique are adopted to convexify non-convex inequality constraints.

(2) A specific quadric form performance index relative to angular velocity is provided to ensure the accuracy of the transformation.

(3) The proposed algorithm is extensible, indicating that the range and the number of constraints can be easily adjusted.

The remainder of this paper is organized as follows: Section 1 demonstrates the mathematical description of the constrained spacecraft reorientation problem. Section 2 provides the convexification and relaxation of the problem, then the successive SOCP algorithm is proposed. In section 3, the numerical simulation is provided, and the conclusions is detailed in section 4.

1 Optimal Control Problem Statement

In this section, the spacecraft orientation in the body frame B relative to the inertial frame I is represented by Euler angle in a 1-2-3 sequence. Then, the mathematical descriptions of the constraints of the spacecraft reorientation problem are formulated. Finally, the formulation of the original optimal attitude reorientation problem is given.

1.1 Kinematic and dynamic model

Consider the attitude kinematics of a rigid spacecraft described by Euler angle[8]

$$\begin{cases} \dot{\varphi} = (\omega_x \cos\psi - \omega_y \sin\psi)/\cos\theta \\ \dot{\theta} = \omega_x \sin\psi + \omega_y \cos\psi \\ \dot{\psi} = \omega_z - (\omega_x \cos\psi - \omega_y \sin\psi)\tan\theta \end{cases} \quad (1)$$

And the dynamic model can be described as

$$\begin{cases} \dot{\omega}_x = \omega_y \omega_z (I_y - I_z)/I_x + M_x/I_x \\ \dot{\omega}_y = \omega_x \omega_z (I_z - I_x)/I_y + M_y/I_y \\ \dot{\omega}_z = \omega_x \omega_y (I_x - I_y)/I_z + M_z/I_z \end{cases} \quad (2)$$

where φ, θ, ψ denote the roll, the pitch and the yaw angles of the spacecraft; $\omega_x, \omega_y, \omega_z$ the angular velocities around the body axes; M_x, M_y, M_z the control torque; and I_x, I_y, I_z the diagonal values of the inertial matrix. And it makes no difference for the optimal problem given in this paper even if the matrix is not diagonal.

Define $\boldsymbol{y} = [\varphi\ \theta\ \psi\ \omega_x\ \omega_y\ \omega_z]$ as the state vector, and the control vector is represented by $\boldsymbol{u} = [M_x\ M_y\ M_z]$. Thus, the nonlinear state equation can be governed as

$$\dot{\boldsymbol{y}} = f(\boldsymbol{y}, \boldsymbol{u}) \quad (3)$$

1. 2　Constraints of the problem

The mathematical descriptions of the initial and the terminal constrains, the attitude forbidden constraints, the angular velocity saturation and the actuator saturation are given bellow.

Firstly, the initial and the terminal constrains are provided

$$\begin{cases} \boldsymbol{y}(t_0) = \boldsymbol{y}_0,\ \boldsymbol{y}(t_f) = \boldsymbol{y}_f \\ \boldsymbol{u}(t_0) = \boldsymbol{u}_0,\ \boldsymbol{u}(t_f) = \boldsymbol{u}_f \end{cases} \quad (4)$$

where t_0 and t_f represent the initial and the terminal moments, respectively.

The saturation constraints, including the angular velocity saturation and the actuator saturation, can be formulated as

$$\begin{cases} -\omega_{\max} \leqslant \omega_x \leqslant \omega_{\max} \\ -\omega_{\max} \leqslant \omega_y \leqslant \omega_{\max} \\ -\omega_{\max} \leqslant \omega_z \leqslant \omega_{\max} \end{cases} \quad (5)$$

$$\begin{cases} -M_{\max} \leqslant M_x \leqslant M_{\max} \\ -M_{\max} \leqslant M_y \leqslant M_{\max} \\ -M_{\max} \leqslant M_z \leqslant M_{\max} \end{cases} \quad (6)$$

where $\omega_{\max}$ represents the maximum value of the an-

gular velocity, and $M_{\max}$ the maximum control torque that actuators can provide.

Subsequently, the mathematical descriptions of attitude forbidden constraints are given as following. The transformation matrix under 1-2-3 rotation of Euler angle is given by

$$\boldsymbol{R} = \begin{bmatrix} c\theta c\psi & s\varphi s\theta c\psi + c\varphi s\psi & -c\varphi c\psi s\theta + s\varphi s\psi \\ -c\theta s\psi & -s\varphi s\theta s\psi + c\varphi c\psi & c\varphi s\theta s\psi + s\varphi c\psi \\ s\theta & -s\varphi c\theta & c\varphi c\theta \end{bmatrix}$$

$$(7)$$

where $c(\cdot) \triangleq \cos(\cdot)$ and $s(\cdot) \triangleq \sin(\cdot)$.

Suppose that $\boldsymbol{n}_s^B$ is a unit vector in the body frame, which represents the boresight vector (the pointing of the sensing instrument). $\boldsymbol{n}_o^I$ is defined as the unit forbidden vector which points toward the obstacle in the inertial frame, and β represents the keep-out angle. Thus, the attitude forbidden zone constraint can be described as[26]

$$\boldsymbol{R} \cdot \boldsymbol{n}_s^B \cdot \boldsymbol{n}_o^I \leqslant \cos\beta \quad (8)$$

It is assumed that the sensing instrument is align with Z axis of the body frame, i. e. $\boldsymbol{n}_o^I = [0, 0, 1]$. Given any boresight vector $\boldsymbol{n}_s^B = [X_0, Y_0, Z_0]$, the attitude forbidden zone constraint can be rewritten as

$$X_0 \sin\theta - Y_0 \sin\varphi \cos\theta + Z_0 \cos\varphi \cos\theta \leqslant \cos\beta \ (9)$$

In order to avoid the singularity in the kinematics Eq.(1), the following constraint is introduced

$$-\sin(\pi/2 - \sigma) \leqslant \sin\theta \leqslant \sin(\pi/2 - \sigma) \quad (10)$$

where σ is a small positive constant.

1. 3　Optimal control problem formulation

The optimal control problem considered in this paper is to obtain the solution subject to attitude dynamics and physical constraints, so that the trajectory of the spacecraft will start from the initial condition and finally arrive at the desired terminal condition, while minimizing the proposed quadric form performance index relative to the angular velocity

$$F = \int_{t_0}^{t_f} \kappa \mathrm{d}t \quad (11)$$

where $\kappa = \varepsilon_1 \omega_x^2 + \varepsilon_2 \omega_y^2 + \varepsilon_3 \omega_z^2$, and $\varepsilon_i\ (i = 1, 2, 3)$

are positive weighting coefficients.

Therefore, the optimal control problem can be stated

$$\boldsymbol{P}_0: \qquad \min F = \int_{t_0}^{t_f} \kappa \mathrm{d}t$$

Subject to   Eqs.(3—6,9,10)

2 Convexification and Relaxation

Due to the strong nonlinearity and non-convexity of the original optimal control problem, convexification and relaxation are adopted to cast the original optimal problem into the SOCP framework. In particular, the equivalence of the transformations is certified. Finally, a successive SOCP algorithm is provided to solve the problem iteratively.

2. 1 Transformation of state equation

Since the SOCP frame requires linear state equation, the mathematical model (3) is supposed to be transformed by variable substitution

$$\begin{cases} \dot{u}_{12} = -\dfrac{u_{11}u_{32}}{u_{22}}\omega_x + \dfrac{u_{11}u_{31}}{u_{22}}\omega_y \\[2mm] \dot{u}_{22} = -u_{21}u_{31}\omega_x - u_{21}u_{32}\omega_y \\[2mm] \dot{u}_{32} = -u_{31}\omega_z + \dfrac{u_{21}u_{31}u_{32}}{u_{22}}\omega_x - \dfrac{u_{21}u_{31}^2}{u_{22}}\omega_y \end{cases} \quad (12)$$

where $u_{11} = \sin\varphi$, $u_{12} = \cos\varphi$, $u_{21} = \sin\theta$, $u_{22} = \cos\theta$, $u_{31} = \sin\psi$, $u_{32} = \cos\psi$.

These variables are not independent, then a new constraint is introduced

$$\begin{cases} u_{11}^2 + u_{12}^2 = 1 \\ u_{21}^2 + u_{22}^2 = 1 \\ u_{31}^2 + u_{32}^2 = 1 \end{cases} \quad (13)$$

In the transformed state equation, the new control vector is defined as $\boldsymbol{\nu} = [u_{11}\ u_{21}\ u_{31}\ M_x\ M_y\ M_z]$, and the new state vector is $\boldsymbol{x} = [u_{12}\ u_{22}\ u_{32}\ \omega_x\ \omega_y\ \omega_z]$. And the nonlinear state equation can be rewritten as

$$\dot{\boldsymbol{x}} = \boldsymbol{g}(\boldsymbol{x},\boldsymbol{\nu}) \qquad (14)$$

Let $(\boldsymbol{x}^k,\boldsymbol{\nu}^k)$ denotes the kth solution in the iterations, then the equation is linearized by standard Taylor series expansion

$$\dot{\boldsymbol{x}} = \frac{\partial \boldsymbol{g}}{\partial \boldsymbol{x}}(\boldsymbol{x}^k)(\boldsymbol{x} - \boldsymbol{x}^k) + \frac{\partial \boldsymbol{g}}{\partial \boldsymbol{v}}(\boldsymbol{v}^k)(\boldsymbol{v} - \boldsymbol{v}^k) - \boldsymbol{g}(\boldsymbol{x}^k,\boldsymbol{v}^k)$$

(15)

Thus, the non-convex and nonlinear state equation is converted into the linear one, which meets the SCOP requirement. And it has the following form after rearrangement

$$\dot{\boldsymbol{x}} = \boldsymbol{A}(\boldsymbol{x}^k,\boldsymbol{\nu}^k)\boldsymbol{x} + \boldsymbol{B}(\boldsymbol{x}^k,\boldsymbol{\nu}^k)\boldsymbol{\nu} + \boldsymbol{c}(\boldsymbol{x}^k,\boldsymbol{\nu}^k) \quad (16)$$

where $\quad \boldsymbol{c} = [\begin{matrix} c_1 & c_2 & c_3 & c_4 & c_5 & c_6 \end{matrix}]^{\mathrm{T}}, \qquad \boldsymbol{A} =$

$$\begin{bmatrix} 0 & a_{12} & a_{13} & a_{14} & a_{15} & 0 \\ 0 & 0 & a_{23} & a_{24} & a_{25} & 0 \\ 0 & a_{32} & a_{33} & a_{34} & a_{35} & a_{36} \\ 0 & 0 & 0 & 0 & a_{45} & a_{46} \\ 0 & 0 & 0 & a_{54} & 0 & a_{56} \\ 0 & 0 & 0 & a_{64} & a_{65} & 0 \end{bmatrix}, \boldsymbol{B} = \begin{bmatrix} b_{11} & 0 & b_{13} & 0 & 0 & 0 \\ 0 & b_{22} & b_{23} & 0 & 0 & 0 \\ 0 & b_{32} & b_{33} & 0 & 0 & 0 \\ 0 & 0 & 0 & b_{44} & 0 & 0 \\ 0 & 0 & 0 & 0 & b_{55} & 0 \\ 0 & 0 & 0 & 0 & 0 & b_{66} \end{bmatrix}.$$

To guarantee the validity of the above linearization, a trust-region constraint is considered

$$\left| (\boldsymbol{x},\boldsymbol{\nu}) - (\boldsymbol{x}^k,\boldsymbol{\nu}^k) \right| \leqslant \boldsymbol{\varsigma} \qquad (17)$$

where $\boldsymbol{\varsigma}$ is a constant vector.

2. 2 Convexification of non-convex constraints

After the above control augmentation, there have been some changes in the constraints described in the previous section. Firstly, the initial and the terminal constraints in Eq.(4) are transformed as

$$\begin{cases} \boldsymbol{x}(t_0) = \boldsymbol{x}_0, \ \ \boldsymbol{x}(t_f) = \boldsymbol{x}_f \\ \boldsymbol{\nu}(t_0) = \boldsymbol{\nu}_0, \ \ \boldsymbol{\nu}(t_f) = \boldsymbol{\nu}_f \end{cases} \qquad (18)$$

And the constraint in Eq.(10) becomes

$$-\sin(\pi/2 - \sigma) \leqslant u_{21} \leqslant \sin(\pi/2 - \sigma) \quad (19)$$

The attitude forbidden zone constraint in Eq.(9) can be rewritten as

$$X_0 u_{21} - Y_0 u_{11} u_{22} + Z_0 u_{12} u_{22} \leqslant \cos\beta \qquad (20)$$

where σ is a small positive constant.

However, the SOCP framework can only deal with the linear equality constraints and the second-order cone inequality constraints. Obviously, the constraint in Eq.(20) is supposed to be further linearized

$$-Y_0 u_{22}^k u_{11} + Z_0 u_{22}^k u_{12} + X_0 u_{21} + (-Y_0 u_{11}^k + $$
$$Z_0 u_{12}^k)u_{22} + Y_0 u_{11}^k u_{22}^k - Z_0 u_{12}^k u_{22}^k - \cos\beta \leqslant 0 \quad (21)$$

To make sure that the spacecraft could avoid the attitude forbidden zone, one can transform

Eq.(21) into

$$-Y_0 u_{22}^k u_{11} + Z_0 u_{22}^k u_{12} + X_0 u_{21} + (-Y_0 u_{11}^k +$$
$$Z_0 u_{12}^k) u_{22} + Y_0 u_{11}^k u_{22}^k - Z_0 u_{12}^k u_{22}^k - \cos(\beta + \delta) \leqslant 0$$

$$(22)$$

where δ is a small positive constant.

Besides, constraint in Eq.(13) is obviously non-convex, which cannot meet SOCP requirement certainly. But the result will not be accuracy if the same convex approximation that is applied to the attitude forbidden constraint is employed. However, another convexification technique is utilized to relax the constraint in Eq.(13) to expand its feasible set, so that it becomes convex. Concretely, it is relaxed to be a second-order inequality constraint directly

$$\begin{cases} u_{11}^2 + u_{12}^2 \leqslant 1 \\ u_{21}^2 + u_{22}^2 \leqslant 1 \\ u_{31}^2 + u_{32}^2 \leqslant 1 \end{cases} \qquad (23)$$

Although the transformation does not seem equivalent, the objective function F can guarantee that the constraint in Eq.(23) is active almost everywhere, which means that Eq.(13) can be satisfied. And the detailed demonstration will be provided in the following section.

Now the optimization problem has been put into to the SOCP framework, described as

$$P_1: \qquad \min F = \int_{t_0}^{t_f} \kappa \mathrm{d}t$$

Subject to   Eqs.(5,6,16—19,22,23)

2.3 L1-penalized relaxation

Since the inappropriate guess of the initial path may cause the violation of attitude forbidden constraints, L1 penalty method is utilized to solve this issue.

Non-negative slack variables are introduced to Eq.(22)

$$-Y_0 u_{22}^k u_{11} + Z_0 u_{22}^k u_{12} + X_0 u_{21} + (-Y_0 u_{11}^k +$$
$$Z_0 u_{12}^k) u_{22} + Y_0 u_{11}^k u_{22}^k - Z_0 u_{12}^k u_{22}^k - \cos(\beta + \delta) +$$
$$\mu_1 - \mu_2 \leqslant 0 \qquad (24)$$

$$\mu_1 \geqslant 0, \mu_2 \geqslant 0 \qquad (25)$$

And the objective function can be modified as

$$F' = \int_{t_0}^{t_f} \kappa \mathrm{d}t + \varepsilon_4 \int_{t_0}^{t_f} (\mu_1 + \mu_2) \mathrm{d}t \qquad (26)$$

where ε_4 is a large constant.

With the above transformation, the optimal control problem becomes

$$P_2: \qquad \min F' = \int_{t_0}^{t_f} \kappa \mathrm{d}t + \varepsilon_4 \int_{t_0}^{t_f} (\mu_1 + \mu_2) \mathrm{d}t$$

Subject to   Eqs.(5,6,16—19,23—25)

Then the assurance of the active constraint in Eq.(23) will be demonstrated as follows.

Assumption 1   The constraint in Eq.(23) is inactive, which means that $|(x, \nu) - (x^k, \nu^k)| < \varsigma$ always holds.

Remark 1   In fact, Assumption 1 is almost satisfied as the problem is not divergent and a proper ς is chosen.

Theorem 1   Let (x^*, ν^*) be the optimal solution of P_2 over a fixed interval $[t_0, t_f]$. then the constraint in Eq.(23) will be active almost everywhere.

Proof   See the Appendix.

Remark 2   If there are more than one attitude forbidden constraints in the problem, Theorem 1 will still be hold with the similar proof.

2.4 Successive SOCP algorithm

The constrained attitude reorientation problem of rigid spacecraft has been cast into an SOCP framework, then it is supposed to be discretized to several iteratively solved problems[27-29]. $N+1$ represents the number of the discrete time points, and the time step size is defined as $\Delta t = t_f / N$.

$$P_3^k: \min F' = \sum_{i=1}^{N+1} (\varepsilon_1 \omega_{xi}^2 + \varepsilon_2 \omega_{yi}^2 + \varepsilon_3 \omega_{zi}^2) t +$$
$$(\mu_{1i} + \mu_{2i}) \Delta t$$
Subject to

$$\frac{x_{i+1} - x_i}{\Delta t} = A(x_i^k, \nu_i^k) x_i + B(x_i^k, \nu_i^k) \nu_i + c(x_i^k, \nu_i^k)$$

$$(27)$$

$$x_1 = x_0, \ x_{N+1} = x_f, \nu_1 = \nu_0, \nu_{N+1} = \nu_f \qquad (28)$$

$$\begin{cases} -\omega_{max} \leqslant \omega_{xi} \leqslant \omega_{max}, \\ -\omega_{max} \leqslant \omega_{yi} \leqslant \omega_{max}, \\ -\omega_{max} \leqslant \omega_{zi} \leqslant \omega_{max} \end{cases} \qquad (29)$$

$$\begin{cases} -M_{\max} \leqslant M_{xi} \leqslant M_{\max}, \\ -M_{\max} \leqslant M_{yi} \leqslant M_{\max}, \\ -M_{\max} \leqslant M_{zi} \leqslant M_{\max} \end{cases} \quad (30)$$

$$u_{11i}^2 + u_{12i}^2 \leqslant 1, u_{21i}^2 + u_{22i}^2 \leqslant 1, u_{31i}^2 + u_{32i}^2 \leqslant 1 \quad (31)$$

$$-Y_0 u_{22i}^k u_{11i} + Z_0 u_{22i}^k u_{12i} + X_0 u_{21i} + (-Y_0 u_{11i}^k + Z_0 u_{12i}^k) u_{22i} + Y_0 u_{11i}^k u_{22i} - Z_0 u_{12i}^k u_{22i} - \cos(\beta + \delta) + \mu_{1i} - \mu_{2i} \leqslant 0 \quad (32)$$

$$\mu_{1i} \geqslant 0, \mu_{2i} \geqslant 0 \quad (33)$$

$$-\sin(\pi/2 - \sigma) \leqslant u_{21i} \leqslant \sin(\pi/2 - \sigma)$$

$$i = 1, \cdots, N \quad (34)$$

where the number of iterations is depicted by the superscript k, and the subscript i denotes the ith discrete point.

Then the successive SOCP algorithm will be given.

Algorithm

Input: initial and terminal states, boundaries, attitude forbidden zones

Select: ε_i ($i = 1, 2, 3, 4$), ς_i ($i = 1, 2$), $\sigma, \delta, n_{sc}, \beta_r, \beta_v$

Output: $(\boldsymbol{x}^*, \boldsymbol{\nu}^*)$

S1: set $k = 1$

Select an initial reference path $(\boldsymbol{x}^k, \boldsymbol{\nu}^k)$;

S2: while $k = 2$

Solve P_3^k with ς_1 to get $(\boldsymbol{x}^k, \boldsymbol{\nu}^k)$;

S3: while $k > 2$

Solve P_3^k with ς_2 to get $(\boldsymbol{x}^k, \boldsymbol{\nu}^k)$;

Calculate $\beta_v^k = \left| \sum_{i=1}^{N} (\mu_{1i}^k + \mu_{2i}^k) \Delta t \right|$

$\beta_r^k = \sum_{i=1}^{N+1} (\omega_{xi}^k - \omega_{xi}^{k-1})^2 + (\omega_{yi}^k - \omega_{yi}^{k-1})^2 + (\omega_{yi}^k - \omega_{yi}^{k-1})^2$

If $\beta_r^k \leqslant \beta_r$ & $\beta_v^k \leqslant \beta_v$ or $k \geqslant n_{sc}$

end while

$(\boldsymbol{x}^*, \boldsymbol{\nu}^*) = (\boldsymbol{x}^k, \boldsymbol{\nu}^k)$

else

set $k = k + 1$

end

end

Here ς_2 is a sufficiently small constant vector to guarantee constraint in Eq.(23) is active approximately.

3 Numerical Simulation

In this section, numerical simulations are conducted to validate the effectiveness of the proposed spacecraft reorientation scheme. The algorithm is solved in MATLAB using YALMI[30] and MOSEK[31], which could solve standard SOCP problems rapidly.

The spacecraft parameters in the simulation are provided as: $I_x = 300 \, \text{kg} \cdot \text{m}^2, I_y = 200 \, \text{kg} \cdot \text{m}^2, I_z = 190 \, \text{kg} \cdot \text{m}^2$. The desired attitude is $(0°, 0°, 0°)$, and the initial attitude is $(-72.364\,6°, 0.034\,4°, 27.381\,7°)$. The maneuver time is set as $150 \, \text{s}$. The saturation constraints of the angular velocity and control torque are restricted as $0.1 \, \text{rad/s}$ and $3 \, \text{N} \cdot \text{m}$, respectively.

Since the iteration algorithm requires initial values, the initial maneuver path is supposed to be provided. Various method can be employed to obtain the initial path. For simplicity, a PD controller in Ref.[32] is applied in the simulation, which does not consider saturation constraints and attitude forbidden constraints.

3.1 Reorientation with single attitude forbidden zone

In scenario 1, only one attitude forbidden zone is considered. The forbidden vector is assumed as $[0.113\,8, 0.350\,1, 0.929\,8]$, and the keep-out angle is $11°$.

Fig.1 shows the 3-D path of the spacecraft, in which the cone represents the attitude forbidden zone. Although the initial path provided by PD controller violates the forbidden zone, the optimal path obtained by iteration can reach the desired attitude successfully while avoiding the attitude forbidden zone. And the projection (2-D path) is presented in Fig.2.

The state and control variables of the spacecraft are shown in Figs.3—5. It can be seen in Fig.3 that the Euler angles are driven to their desired terminal values. The angular velocity and the control
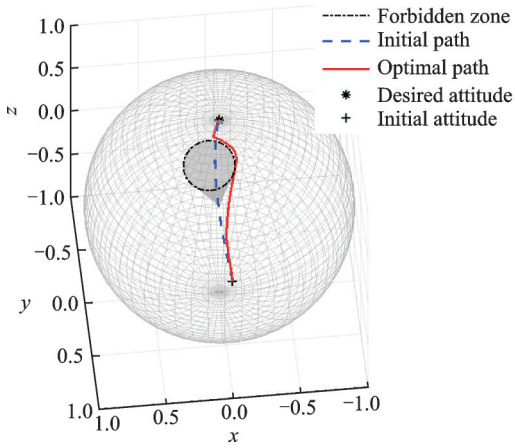
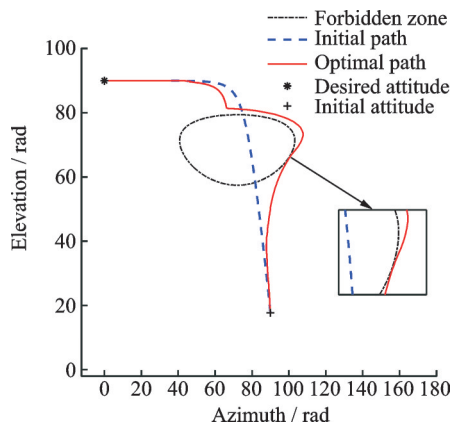Fig.1   3-D path of the spacecraft in scenario 1

Fig.2   2-D path of the spacecraft in scenario 1
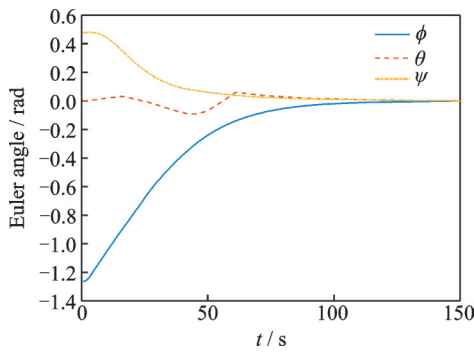

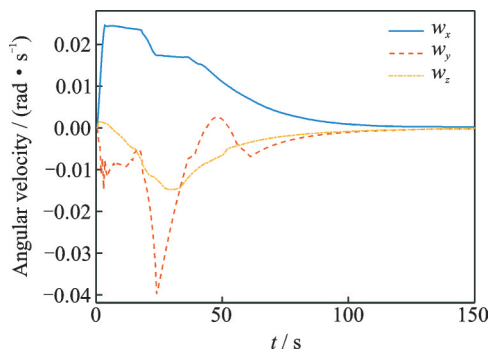Fig.3   Euler angles in scenario 1

Fig.4   Angular velocities in scenario 1

torque are depicted in Fig.4 and Fig.5, respectively. As shown in Fig.6 the constraint in Eq.(23) is active during maneuvering.
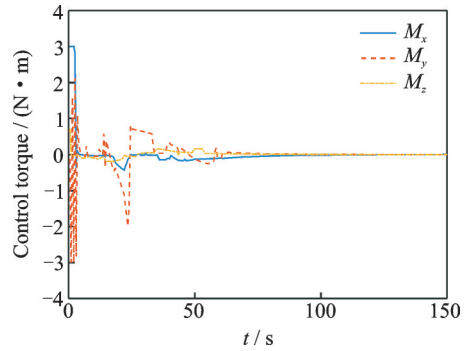

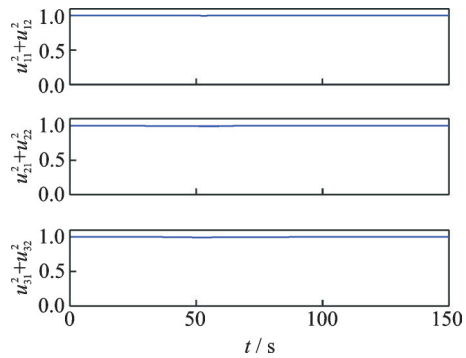Fig.5   Control torques in scenario 1

Fig.6   Constraint in Eq.(23) in scenario 1

3.2   Reorientation with multiple attitude forbidden zones

In scenario 2, two attitude forbidden zones are considered. Specifically, the forbidden vectors are set as $[-0.068\,98, 0.361\,6, 0.929\,8]$ and $[0.291\,5, 0.619\,4, 0.729\,0]$, the keep-out angles are $11°$ and $15°$, respectively.

Also, to demonstrates the superiority of the designed algorithm, the artificial potential function-based controller in Ref.[1] is simulated for comparison. The comparison results under the two algorithms are shown in Fig.7. Although both paths can avoid two attitude forbidden zones and then reach the desired attitude. The path generated by APF is much longer than the path obtained by the proposed control scheme, which means the proposed control scheme requires less consumption. And the corresponding 2-D path of the spacecraft is provided by Fig.8. The saturation constraints and the constraint
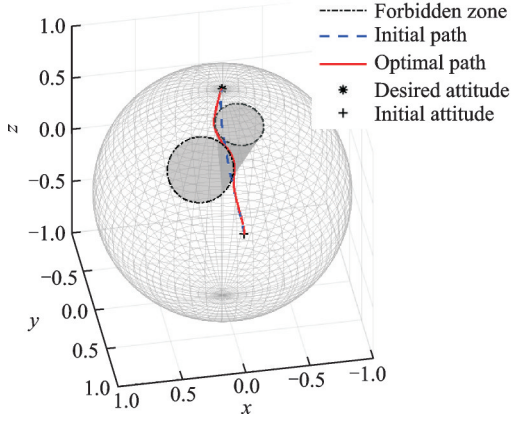
in Eq. (23) are also guaranteed, as shown in Figs.9—12.

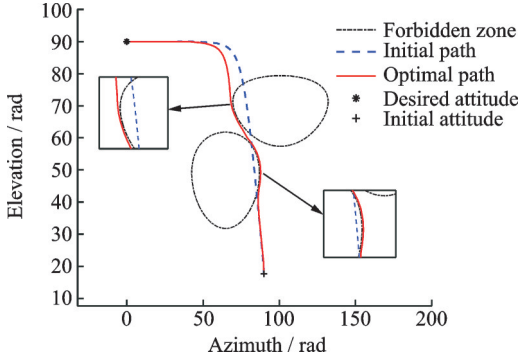

Fig.7   3-D path of the spacecraft in scenario 2

Fig.8   2-D path of the spacecraft in scenario2
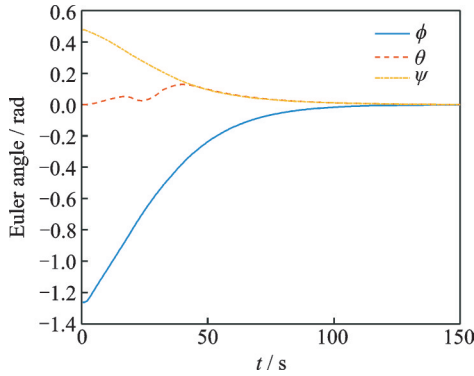

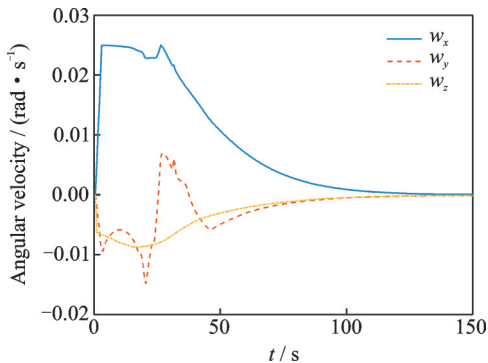Fig.9   Euler angles in scenario 2

Fig.10   Angular velocities in scenario 2
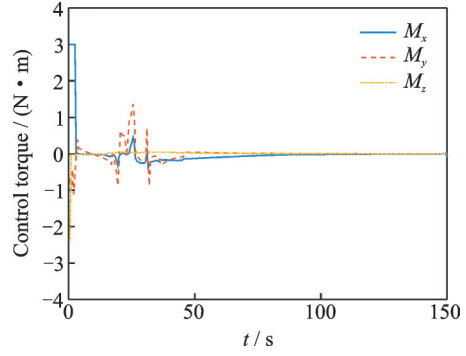

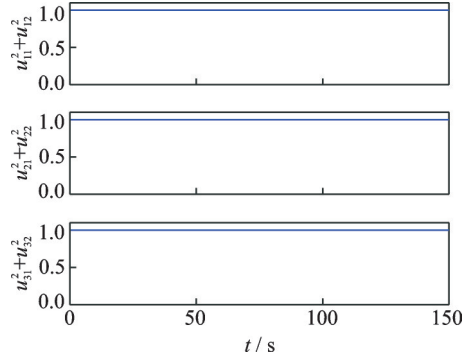Fig.11   Control torques in scenario 2

Fig.12   Constraint in Eq.(23) in scenario 2

4   Conclusions

A successive SOCP algorithm is conducted to address the reorientation problem of rigid spacecraft in the presence of saturation constraints and attitude forbidden constraints. The core part of this paper consists of two parts: (1) The original nonlinear and non-convex constrained reorientation problem is transformed into a standard SOCP problem by convexification and relaxation; (2) the specific quadratic-form performance index relative to angular velocity can guarantee the equivalence of transformations. Finally, the algorithm is verified by a numerical simulation. Further research will focus on the convergence analysis of the iteration.

Appendix: Proof of Proposition 1

The Hamiltonian of P_2 is defined

$$
\begin{aligned}
H = & P_0 [\varepsilon_1 \omega_x^2 + \varepsilon_2 \omega_y^2 + \varepsilon_3 \omega_z^2 + \varepsilon_4 (\mu_1 + \mu_2)] + \\
& P_1 (a_{12} u_{22} + a_{13} u_{32} + a_{14} \omega_x + a_{15} \omega_y + b_{11} u_{11} + \\
& b_{13} u_{31} + c_1) + P_2 (a_{23} u_{32} + a_{24} \omega_x + a_{25} \omega_y + \\
& b_{22} u_{21} + b_{23} u_{31} + c_2) + P_3 (a_{32} u_{22} + a_{33} u_{32} + \\
& a_{34} \omega_x + a_{35} \omega_y + a_{36} \omega_z + b_{32} u_{21} + b_{33} u_{31} + \\
& c_3) + P_4 (a_{45} \omega_y + a_{46} \omega_z + b_{44} M_x + c_4) + \\
& P_5 (a_{54} \omega_x + a_{56} \omega_z + b_{55} M_y + c_5) + \\
& P_6 (a_{64} \omega_x + a_{65} \omega_y + b_{66} M_z + c_6) \qquad (A1)
\end{aligned}
$$

The Lagrangian of P_2 is derived as

$$L = H + \lambda_1^-(\omega_{max} + \omega_x) + \lambda_1^+(\omega_{max} - \omega_x) +$$
$$\lambda_2^-(\omega_{max} + \omega_y) + \lambda_2^+(\omega_{max} - \omega_y) + \lambda_3^-(\omega_{max} +$$
$$\omega_z) + \lambda_3^+(\omega_{max} - \omega_z) + \lambda_4^-(M_{max} + M_x) +$$
$$\lambda_4^+(M_{max} - M_x) + \lambda_5^-(M_{max} + M_y) +$$
$$\lambda_5^+(M_{max} - M_y) + \lambda_6^-(M_{max} + M_z) +$$
$$\lambda_6^+(M_{max} - M_z) + \lambda_7(1 - u_{11}^2 - u_{12}^2) + \lambda_8(1 -$$
$$u_{21}^2 - u_{22}^2) + \lambda_9(1 - u_{31}^2 - u_{32}^2) + \lambda_{10}\mu_1 +$$
$$\lambda_{11}\mu_2 + \lambda_{12}(Y_0 u_{22}^k u_{11} - Z_0 u_{22}^k u_{12} - X_0 u_{21} +$$
$$(Y_0 u_{11}^k - Z_0 u_{12}^k) u_{22} - Y_0 u_{11}^k u_{22}^k + Z_0 u_{12}^k u_{22}^k +$$
$$\cos(\beta + \varepsilon) - \mu_1 + \mu_2) + \lambda_{13}^-(u_{21} + \sin(\pi/2 -$$
$$\sigma)) + \lambda_{13}^+(u_{21} - \sin(\pi/2 - \sigma)) \qquad (A2)$$

Thus

(1) The nontriviality condition

$$[P_0\ P_1\ P_2\ P_3\ P_4\ P_5\ P_6] \neq 0 \quad \forall t \in [t_0, t_f] \quad (A3)$$

(2) The costate differential equations

$$P_1' = -\frac{\partial L}{\partial u_{12}} = -(-2\lambda_7 u_{12} - \lambda_{12} Z_0 u_{22}^k) \qquad (A4)$$

$$P_2' = -\frac{\partial L}{\partial u_{22}} = -(P_1 a_{12} + P_2 a_{32} - 2\lambda_8 u_{22} +$$
$$\lambda_{12}(Y_0 u_{11}^k - Z_0 u_{12}^k)) \qquad (A5)$$

$$P_3' = -\frac{\partial L}{\partial u_{32}} = -(P_1 a_{13} + P_2 a_{23} + P_3 a_{33} - 2\lambda_8 u_{22})$$
$$\qquad (A6)$$

$$P_4' = -\frac{\partial L}{\partial \omega_x} = -(2P_0\varepsilon_1\omega_x + P_1 a_{14} + P_2 a_{24} +$$
$$P_3 a_{34} + P_5 a_{54} + P_6 a_{64} + \lambda_1^- - \lambda_1^+) \qquad (A7)$$

$$P_5' = -\frac{\partial L}{\partial \omega_y} = -(2P_0\varepsilon_2\omega_y + P_1 a_{15} + P_2 a_{25} +$$
$$P_3 a_{35} + P_4 a_{45} + P_6 a_{65} + \lambda_2^- - \lambda_2^+) \qquad (A8)$$

$$P_6' = -\frac{\partial L}{\partial \omega_z} = -(2P_0\varepsilon_3\omega_z + P_3 a_{36} + P_4 a_{46} +$$
$$P_5 a_{56} + \lambda_3^- - \lambda_3^+) \qquad (A9)$$

(3) The stationary conditions

$$\frac{\partial L}{\partial u_{11}} = P_1 b_{11} - 2\lambda_7 u_{11} + \lambda_{12} Y_0 u_{22}^k = 0 \quad (A10)$$

$$\frac{\partial L}{\partial u_{21}} = P_2 b_{22} + P_3 b_{32} - 2\lambda_8 u_{21} - \lambda_{12} X_0 +$$
$$\lambda_{13}^- + \lambda_{13}^+ = 0 \qquad (A11)$$

$$\frac{\partial L}{\partial u_{31}} = P_1 b_{13} + P_2 b_{23} + P_3 b_{33} - 2\lambda_9 u_{31} = 0 (A12)$$

$$\frac{\partial L}{\partial M_x} = P_4 b_{44} + \lambda_4^- - \lambda_4^+ = 0 \qquad (A13)$$

$$\frac{\partial L}{\partial M_y} = P_5 b_{55} + \lambda_5^- - \lambda_5^+ = 0 \qquad (A14)$$

$$\frac{\partial L}{\partial M_z} = P_6 b_{66} + \lambda_6^- - \lambda_6^+ = 0 \qquad (A15)$$

(4) The Karush-Kuhn-Tucker conditions

$$\lambda_1^- \geqslant 0, \lambda_1^-(\omega_{max} + \omega_x) = 0$$
$$\lambda_1^+ \geqslant 0, \lambda_1^+(\omega_{max} - \omega_x) = 0 \qquad (A16)$$
$$\lambda_2^- \geqslant 0, \lambda_2^-(\omega_{max} + \omega_y) = 0$$
$$\lambda_2^+ \geqslant 0, \lambda_2^+(\omega_{max} - \omega_y) = 0 \qquad (A17)$$
$$\lambda_3^- \geqslant 0, \lambda_3^-(\omega_{max} + \omega_z) = 0$$
$$\lambda_3^+ \geqslant 0, \lambda_3^+(\omega_{max} - \omega_z) = 0 \qquad (A18)$$
$$\lambda_4^- \geqslant 0, \lambda_4^-(M_{max} + M_x) = 0$$
$$\lambda_4^+ \geqslant 0, \lambda_4^+(M_{max} - M_x) = 0 \qquad (A19)$$
$$\lambda_5^- \geqslant 0, \lambda_5^-(M_{max} + M_y) = 0$$
$$\lambda_5^+ \geqslant 0, \lambda_5^+(M_{max} - M_y) = 0 \qquad (A20)$$
$$\lambda_6^- \geqslant 0, \lambda_6^-(M_{max} + M_z) = 0$$
$$\lambda_6^+ \geqslant 0, \lambda_6^+(M_{max} - M_z) = 0 \qquad (A21)$$
$$\lambda_7 \geqslant 0, \lambda_7(1 - u_{11}^2 - u_{12}^2) = 0 \qquad (A22)$$
$$\lambda_8 \geqslant 0, \lambda_8(1 - u_{21}^2 - u_{22}^2) = 0 \qquad (A23)$$
$$\lambda_9 \geqslant 0, \lambda_9(1 - u_{31}^2 - u_{32}^2) = 0 \qquad (A24)$$
$$\lambda_{10} \geqslant 0, \lambda_{10}\mu_1 = 0 \quad \lambda_{11} \geqslant 0, \lambda_{11}\mu_2 = 0 \quad (A25)$$
$$\lambda_{12} \geqslant 0, \lambda_{12}(Y_0 u_{22}^k u_{11} - Z_0 u_{22}^k u_{12} - X_0 u_{21} + (Y_0 u_{11}^k -$$
$$Z_0 u_{12}^k) u_{22} - Y_0 u_{11}^k u_{22}^k + Z_0 u_{12}^k u_{22}^k + \cos(\beta +$$
$$\delta) - \mu_1 + \mu_2) = 0 \qquad (A26)$$
$$\lambda_{13}^- \geqslant 0, \lambda_{13}^-\left[u_{21} + \sin\left(\frac{\pi}{2} - \sigma\right)\right] = 0$$
$$\lambda_{13}^+ \geqslant 0, \lambda_{13}^+\left[u_{21} - \sin\left(\frac{\pi}{2} - \sigma\right)\right] = 0 \quad (A27)$$

If there exists a finite interval $[t_a, t_b] \in [t_0, t_f]$ where the constraint in Eq. (23) is inactive, it will lead to $\lambda_7 = \lambda_8 = \lambda_9 = 0$.

$\lambda_1^- = \lambda_1^+ = \lambda_2^- = \lambda_2^+ = \lambda_3^- = \lambda_3^+ = 0$ will be obtained by Eqs. (A16—A18), and $\lambda_4^- = \lambda_4^+ = \lambda_5^- = \lambda_5^+ = \lambda_6^- = \lambda_6^+ = 0$ will also be received by Eqs. (A19—A21). And as the introduction of the L1 penalty method, $\lambda_{12} = 0$ can be guaranteed.

Then, substituting the above results into the costate differential Eqs. (A4—A9) and the stationary conditions in Eqs. (A10—A15), $[P_0\ P_1\ P_2\ P_3\ P_4\ P_5\ P_6] = 0$ can be received, which contradicts to the nontriviality condition.

In conclusion, there do not exist a finite inter-

val $[t_a, t_b]$ where the constraint in Eq.(23) is inactive.

References

[1] HU Q, CHI B, AKELLA M R. Anti-unwinding attitude control of spacecraft with forbidden pointing constraints[J]. Journal of Guidance, Control, and Dynamics, 2019, 42(4): 822-835.

[2] HU Q, CHI B, AKELLA M R. Reduced attitude control for boresight alignment with dynamic pointing constraints[J]. IEEE Transactions on Mechatronics, 2020, 24(6): 2942-2952.

[3] HU Q, LIU Y, DONG H, et al. Saturated attitude control for rigid spacecraft under attitude constraints[J]. Journal of Guidance, Control, and Dynamics, 2020, 43(9): 1-16.

[4] LEE U, MESBAHI M. Spacecraft reorientation in presence of attitude constraints via logarithmic barrier potentials[C]//Proceedings of American Control Conference (ACC). San Francisco, USA: IEEE 2011: 450-455.

[5] KJELLBERG H C, LIGHTSEY E G. Discretized constrained attitude pathfinding and control for satellites[J]. Journal of Guidance, Control, and Dynamics, 2013, 36(5): 1301-1309.

[6] KJELLBERG H C, LIGHTSEY E G. Discretized quaternion constrained attitude pathfinding[J]. Journal of Guidance, Control, and Dynamics, 2016, 39(3): 713-718.

[7] BIGGS J D, COLLEY L. Geometric attitude motion planning for spacecraft with pointing and actuator constraints[J]. Journal of Guidance Control, and Dynamics, 2016, 39(7): 1669-1675.

[8] GUIGGIANI A, KOLMANOVSKY I, PATRINOS P, et al. Fixed-point constrained model predictive control of spacecraft attitude[C]//Proceedings of American Control Conference (ACC). Chicago, USA: IEEE, 2015: 2317-2322.

[9] BOYD S, VANDENBERGHE L. Convex optimization[M]. California, USA: Cambridge University Press, 2004.

[10] MACHIELSEN K C P. Numerical solution of optimal control problems with state constraints by sequential quadratic programming in function space[D]. Eindhoven, The Netherlands: Technische Universiteit Eindhoven, 1987.

[11] KIM Y, MESBAHI M. Quadratically constrained attitude control via semidefinite programming[J]. IEEE Transactions on Automatic Control, 2004, 49(5): 731-735.

[12] KIM Y, MESBAHI M, SINGH G, et al. On the convex parameterization of constrained spacecraft reorientation[J]. IEEE Transactions on Aerospace and Electronic Systems, 2010, 46(3): 1097-1109.

[13] LIU X, SHEN Z, LU P. Entry trajectory optimization by second-order cone programming[J]. Journal of Guidance, Control, and Dynamics, 2016, 39(2): 227-241.

[14] BLACKMORE L, AÇIKMEŞE B. Minimum landing error powered descent guidance for Mars landing using convex optimization[J]. Journal of Guidance, Control, and Dynamics, 2010, 33(4): 1161-1171.

[15] SUN C, DAI R. Spacecraft attitude control under constrained zones via quadratically constrained quadratic programming[C]//Proceedings of AIAA Guidance, Navigation, and Control Conference. Florida, USA: AIAA, 2015: 1-16.

[16] SUN C, LIU Y C, DAI R, et al. Two approaches for path planning of unmanned aerial vehicles with avoidance zones[J]. Journal of Guidance Control and Dynamics, 2017, 40(8): 2076-2083.

[17] LIU X, LU P. Solving nonconvex optimal control problems by convex optimization[J]. Journal of Guidance Control, and Dynamics, 2014, 37(3): 750-765.

[18] HARRIS M W, AÇIKMEŞE B. Lossless convexification for a class of optimal control problems with linear state constraints[C]//Proceedings of Conference on Decision and Control (CDC). Firenze, Italy: IEEE, 2013: 7113-7118.

[19] RUBIO F R, HARRIS M W, AÇIKMEŞE B. Lossless convexification for a class of optimal control problems with quadratic state constraints[C]//Proceedings of American Control Conference (ACC). Washington, USA: IEEE, 2013: 3415-3420.

[20] HU Q, LI L, FRISWELL M I. Spacecraft anti-unwinding attitude control with actuator nonlinearities and velocity limit[J]. Journal of Guidance Control, and Dynamics, 2015, 38(10): 2042-2050.

[21] HU Q, TAN X. Unified attitude control for spacecraft under velocity and control constraints[J]. Aerospace Science and Technology, 2017, 67: 257-264.

[22] CHEN W, HU Q, GUO L. Anti-unwinding attitude control of rigid spacecraft with angular velocity constraint[C]//Proceedings of Chinese Control Confer-

ence（CCC）. Wuhan, China：IEEE, 2018：9776-9780.

[23] GUPTA R, KALABIĆ U V, CAIRANO S D, et al. Constrained spacecraft attitude control on SO（3）using fast nonlinear model predictive control[C]//Proceedings of American Control Conference（ACC）. Chicago, USA, 2015：2980-2986.

[24] GUIGGIANI A, KOLMANOVSKY I V, PATRINOS P, et al. Constrained model predictive control of spacecraft attitude with reaction wheels desaturation[C]//Proceedings of European Control Conference（ECC）. Austria：[s.n.], 2015：1382-1387.

[25] LEE D Y, GUPTA R, KALABIĆ U V, et al. Geometric mechanics based nonlinear model predictive spacecraft attitude control with reaction wheels[J]. Journal of Guidance Control, and Dynamics, 2017, 40（2）：309-319.

[26] YANG J, DUAN Y, LARBI M, et al. Potential field-based sliding surface design and its application in spacecraft constrained reorientation[J]. Journal of Guidance, Control, and Dynamics, 2020, 44（3）：399-409.

[27] LIU X, LU P. Autonomous trajectory planning for rendezvous and proximity operations by conic optimization[J]. Journal of Guidance, Control, and Dynamics, 2013, 36（2）：375-389.

[28] LIU X, SHEN Z, LU P. Exact convex relaxation for optimal flight of aerodynamically controlled missiles[J]. IEEE Transactions on Aerospace and Electronic Systems, 2016, 52（4）：1881-1892.

[29] CELANI F, LUCARELLI D. Spacecraft attitude motion planning using gradient-based optimization[J]. Journal of Guidance, Control, and Dynamics, 2019, 43（6）：140-145.

[30] LOFBERG J. YALMIP：A toolbox for modeling and optimization in MATLAB[C]//IEEE International Conference on Robotics and Automation. [S. l.]：IEEE, 2004：284-289.

[31] BOYD S, WEGBREIT B. Fast computation of optimal contact forces[J]. IEEE Transactions on Robotics, 2007, 23（6）：1117-1132.

[32] HU Q, TAN X. Unified attitude control for spacecraft under velocity and control constraints[J]. Aerospace Science and Technology, 2017, 67：257-264.

Authors　　Ms. **CHEN Xi** received the B.S. degree in control science and engineering from Harbin Institute of Technology, Harbin, China, in 2018. She is currently working towards the M.S. degree in control science and engineering at Beihang University, Beijing, China. Her research interests include spacecraft motion control and convex optimization.

Prof. **HU Qinglei**（Senior Member, IEEE）received his B. E. degree in electrical and electronic engineering from Zhengzhou University, Zhengzhou, China, in 2001, and Ph.D. degree in guidance and control from Harbin Institute of Technology, Harbin, China, in 2006. From 2003 to 2014, he had been with the Department of Control Science and Engineering at Harbin Institute of Technology and was promoted to the rank of Professor with tenure in 2012. He joined Beihang University, Beijing, China, in 2014, as a full Professor. He worked as a Post-Doctoral Research Fellow in the School of Electrical and Electronic Engineering, Nanyang Technological University, Singapore, from 2006 to 2007, and from 2008 to 2009, he visited the University of Bristol, Bristol, U.K., as a Senior Research Fellow supported by Royal Society Fellowship. After that, he visited Concordia University supported by Natural Sciences and Engineering Research Council of Canada from 2010 to 2011. His research interests include variable structure control and applications, fault-tolerant control and applications. In these areas, he has authored or co-authored over 100 technical papers. He is an Associate Fellow of American Institute of Aeronautics and Astronautics（AIAA）.

Author contributions　　Ms. **CHEN Xi** designed the study, established the mathematical model, and provided the optimization algorithm. Mr. **CAO Ruihao** contributed to the simulation and the analyzation of the study. Prof. **HU Qinglei** contributed to the discussion and background of the study. All authors commented on the manuscript draft and approved the submission.

Competing interests　　The authors declare no compeing interests.

（Production Editor：ZHANG Bei）

基于二阶锥优化的饱和及禁区约束下的航天器姿态控制

陈　曦[1]，曹瑞浩[2]，胡庆雷[1,3]

（1.北京航空航天大学自动化科学与电气工程学院,北京 100191,中国；

2.中航工业集团西安飞行自动控制研究所,西安 710076,中国；

3.北京航空航天大学大数据精准医疗高精尖创新中心,北京 100191,中国）

摘要：研究了姿态禁区约束、角速度和控制力矩饱和约束下的航天器姿态机动问题。为了解决实际问题中的强非线性和非凸问题,提出了采用二阶锥优化方法来求解路径。具体来说,非线性的运动学和动力学通过松弛和转化为标准的仿射形式,并采用线性化和 L1 罚函数方法将问题中的非凸约束进行凸化。提出了基于角速度的二次性能指标,采用逐次迭代的二阶锥优化算法得到航天器姿态机动路径。最终,通过数值仿真验证了算法的有效性。

关键词：航天器姿态机动；姿态禁区约束；执行机构饱和；角速度饱和；二阶锥优化